Correlation between coda Q^{-1} and seismicity in central Japan

By Yoshihiro HIRAMATSU, Masataka ANDO and Fumiaki TAKEUCHI

(Manuscript received on June 24, 1992; received in revised from on Aug. 17, 1992)

Abstract

Coda Q^{-1} is a parameter which represents heterogeneities and stress condition in the lithosphere. We determined coda Q^{-1} in the frequency range from 1.5 to 24 Hz in two areas, the volcanic and the tectonic areas of the Hida region, central Japan. The data were recorded by a telemetering system for events from 1985 to 1991 (367 events), with magnitudes less than 4.0 and depths shallower than 30 km. We found a temporal variation in coda Q^{-1}, the number of earthquakes and b value, all of which increased with time in the volcanic area. However, we could not find significant temporal variation in such values in the tectonic area. Positive correlation between the coda Q^{-1} and the b value was found in the volcanic area, but good correlation was not observed in the tectonic area. We also measured the temporal variation of power of frequency n for coda Q^{-1} defined by the formula $Q_C^{-1} = Q_0^{-1} f^{-n}$, where Q_0^{-1} represents Q_C^{-1} at 1 Hz and f is frequency. The value of n shows no significant temporal change in the Hida region. We consider the cause of the temporal change in coda Q^{-1} in the volcanic area involves aseismic fractures, increasing scatter of creeping cracks, due to magma accumulation.

1. Introduction

The study of coda waves provides information on heterogeneities in the lithosphere. Coda Q^{-1} or Q_C^{-1} is measured from the decay rate of coda wave amplitude of a local earthquake. The coda amplitude decay is independent of the distance and the path between a source and a receiver[1]. The observed general agreement between Q^{-1} of coda waves and Q^{-1} of shear waves in the frequency range $1 \sim 25$ Hz support Aki's[2] hypothesis that the local earthquake S coda is composed primarily of S to S backscattering waves due to heterogeneities distributed more or less uniformly. The values of Q_C^{-1} reported on many regions of the Earth show a remarkable distribution corresponding to tectonic activity. Tectonically active regions show high values of Q_C^{-1} and stable regions show low values. The frequency dependence of Q_C^{-1} is expressed as $Q_0^{-1} f^{-n}$ for frequencies higher than about 1 Hz, where Q_0^{-1} represents Q_C^{-1} at 1 Hz. The value n is also large for active regions ($0.6 \sim 1.0$) and small for stable regions ($0.2 \sim 0.4$). Some typical values of n reported in the literature are given in **Table 1**.

Moreover, since Chouet[5] found a temporal change in Q_C^{-1} in Central California, there have been many reports which show increase or decrease of Q_C^{-1} for local earthquakes before major earthquakes[6][18][8][31][10][23]. Sato[24] also reported that the temporal variation of coda excitation strength related to the Western Nagano Earthquake (Sep. 14, 1984, $M_S = 6.8$) at the south eastern border portion in the Hida region. Relating to occurrence of large earthquakes, the temporal variation in b value was also

Table 1. The power of frequency n for coda Q^{-1} reported in the literature.

Region	n	Reference
New England	0.4	Pulli[15]
Central U.S.	0.20	Singh and Herrmann[27]
Central California (Franciscan)	0.60	Phillips et al.[16]
Central California (Salinian)	0.74	Phillips et al.[16]
Sierra Nevada	1.16	Phillips et al.[16]
Central Asia	0.5	Rautian and Khalturin[17]
Central and eastern Kanto, Japan	0.6	Aki[2]
Northeast Kanto, Japan	0.8	Aki[2]
Adak Island area, central Aleutian	1.05	Scherbaum and Kisslinger[26]
Friulli, Italy	1.1	Rovelli[21]
Central and southcentral Alaska	0.62	Steensma and Biswas[28]
Guam, Mariana Islands	0.46	Jin et al.[12]
Akureyri, Iceland	0.61	Jin et al.[12]

reported[5)10)19)11)]. Good correlation was found between Q_C^{-1} and b value. Some reports show positive correlation while others show negative correlation. These temporal variations in coda Q^{-1} have been suggested as possible precursors to large earthquakes. Since the decrease of Q_C^{-1} possibly corresponds to the closing of cracks, this parameter seems to be a reliable indicator of stress condition[3].
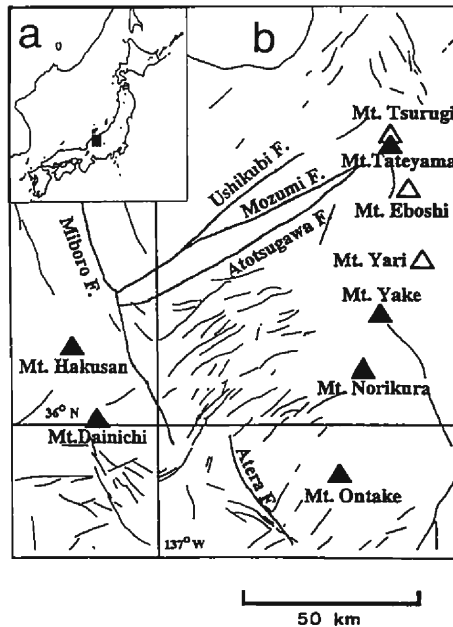

Fig. 1. (a) Solid square shows location of the Hida region. (b) Distribution of active Quaternary faults and active volcanoes. Solid triangles indicate the location of active volcanoes (after Mikumo et al., 1988).

The Hida region, which is located in the northwestern part of the Chubu district, central Honshu, is one of the most active tectonic regions in Japan. In this region, as shown in **Figure 1**, there are many Quaternary faults, such as the Atotsugawa fault, and the Hida mountain range, which contains several active volcanoes aligned from north to south. Prominent low velocity bodies exist just beneath active volcanoes, particularly in the Hida mountain range[9]. This low velocity body can be clearly identified in the crust and the upper mantle.

There have been several large historical earthquakes in and around the present region. One of the largest earthquakes is the 1858 Ansei Hida earthquake with a magnitude of around 7.0, which is believed to have occurred due to the movement of the Atotsugawa fault. Most of the focal mechanisms for earthquakes with magnitudes greater than 3.0 are strike-slip, and the maximum compressive stress inferred from the solutions is oriented in an ESE-WNW direction in this region. This direction appears to be parallel to that of relative motion between the Pacific and Eurasian plates rather than the suggested motion between the North American and Eurasian plates[14].

High seismicity is observed along the Atotsugawa fault and beneath the Hida mountain range. Since 1986, the seismicity has changed in this region and swarm earthquakes have occurred frequently around and beneath the Hida mountain range. In particular from January to April in 1990, the activity of earthquake swarm increased beneath the Hida mountain range. Initially it occurred in the southwest of Mt.
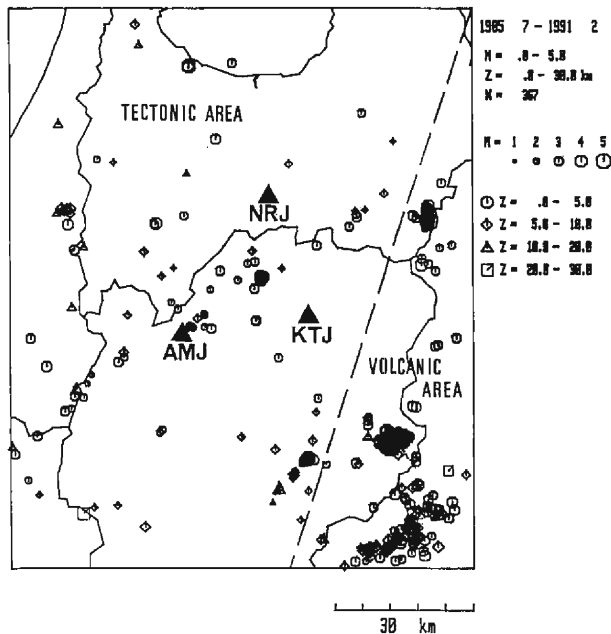

Fig. 2. Epicenters (circles) and stations (triangles) used to calculate Q_C^{-1} in the Hida region. Dashed line divides this region into two areas. The volcanic area contains the Hida mountain range where several active volcanoes are located. The tectonic area contains many Quaternary faults.

Norikura, then gradually migrated to the area around Mt. Yakedake, Mt. Eboshi, and again returned to the east of Mt. Yakedake, the southwest of Mt. Norikura[13)29)].

As mentioned above, the activity of the swarm earthquakes is complex and appears to reflect the stress condition. It can be considered that the stress condition affects the value of $Q_C{}^{-1}$. Since no outstanding earthquake and eruption have occurred in the Hida region in recent years, tectonic stresses and magma supplies have been ac-
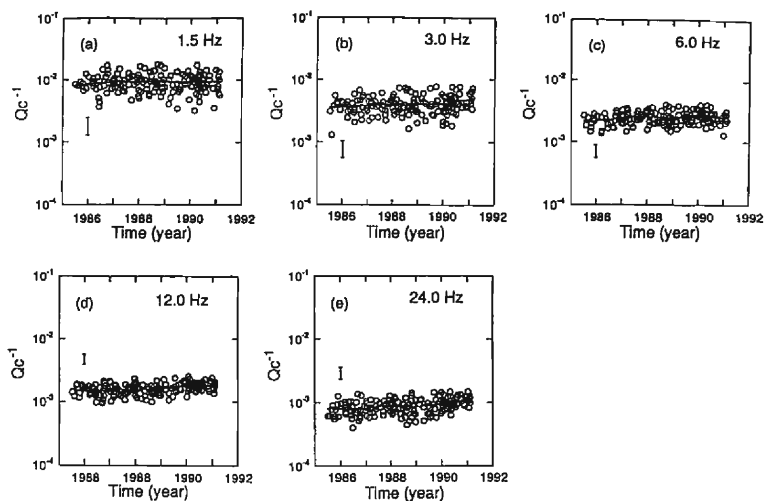

Fig. 3. Temporal variations in $Q_C{}^{-1}$ in the volcanic area at 1.5, 3.0, 6.0, 12.0 and 24.0 Hz. Solid curves represent running mean of 21 successive data and solid bars show standard deviation from the running mean.
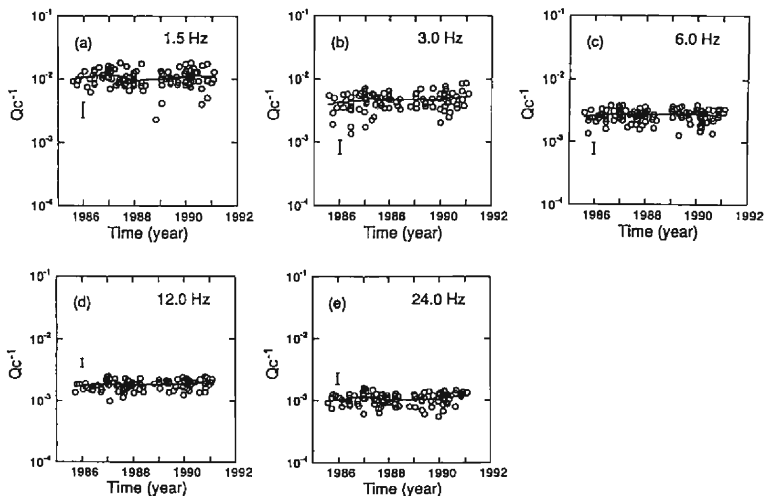

Fig. 4. Temporal variations in $Q_C{}^{-1}$ in the tectonic area at 1.5, 3.0, 6.0, 12.0 and 24.0 Hz. All symbols are the same as those in Fig. 3.

cumulated in this particularly active region. Such readily available data as coda Q^{-1} from the microearthquake observation networks of the Disaster Prevention Research Institute, Kyoto University, provide information on temporal variations of physical properties in the crust and the upper mantle. The present paper purposes to investigate the correlation between seismicity and $Q_C{}^{-1}$ and their temporal change for a long period.

2. Data

The local earthquakes used in this study were recorded at three stations, Amou (AMJ), Nirehara (NRJ), and Kamitakara (KTJ). These stations are a part of the micro-earthquake observation networks and compose the telemetering system called SWARMS (Seismic Wave Automatic Recording and Measuring System) of the Disaster

Table 2. The mean values of $Q_C{}^{-1}$ and the results of statistical test.

|	Mean value			Significance (%)		
	I	II	III	I→II	II→III	I→III
Volcanic area						
1.5 Hz	9.11×10^{-3}	9.38×10^{-3}	9.46×10^{-3}	64.4	88.0	51.5
3.0 Hz	3.87×10^{-3}	4.12×10^{-3}	4.41×10^{-3}	29.0	20.4	1.9
6.0 Hz	2.30×10^{-3}	2.44×10^{-3}	2.66×10^{-3}	19.5	2.7	0.0
12.0 Hz	1.50×10^{-3}	1.55×10^{-3}	1.80×10^{-3}	38.6	0.0	0.0
24.0 Hz	7.98×10^{-4}	8.88×10^{-4}	1.01×10^{-3}	3.0	0.2	0.0
Tectonic area						
1.5 Hz	1.11×10^{-2}	9.81×10^{-3}	1.08×10^{-2}	3.3	12.5	68.3
3.0 Hz	4.50×10^{-3}	4.85×10^{-3}	5.05×10^{-3}	22.0	50.9	11.5
6.0 Hz	2.74×10^{-3}	2.68×10^{-3}	2.76×10^{-3}	64.2	53.9	89.3
12.0 Hz	1.85×10^{-3}	1.77×10^{-3}	1.89×10^{-3}	27.8	6.5	55.3
24.0 Hz	1.15×10^{-3}	1.01×10^{-3}	1.12×10^{-3}	0.2	1.3	55.3
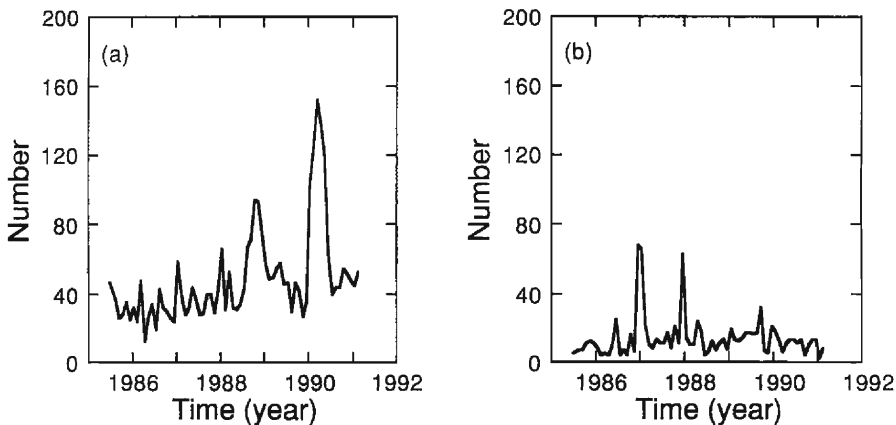
Fig. 5. (a) and (b) indicate temporal variations in the monthly number of earthquakes in the volcanic and the tectonic areas, respectively.

Prevention Research Institute, Kyoto University. This telemetering system was established in 1985 and covers from central to southwest Japan[7]. Since the Hida region is located in the northeast end and earthquakes occur outside of the area covered by this system, the hypocenters determined by SWARMS are often mislocated. To overcome this inadequacy, seismic wave have been exchanged between three stations (Takayama, Yakedake, and Takane) of Nagoya University, which are located in the southeast part of
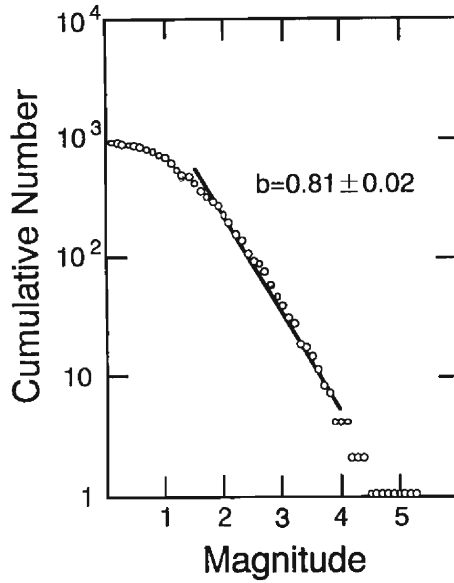

Fig. 6. An example of cumulative frequency distribution of magnitude from Jan. 1986 to Dec. 1986 in the volcanic area. Solid line is drawn by fitting Equation (5) for the magnitiude range of 1.5~4.0.
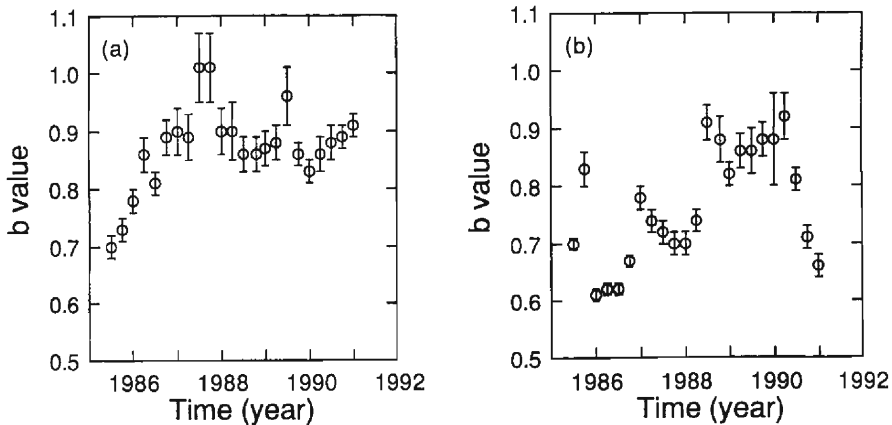

Fig. 7. (a) and (b) indicate temporal variations in *b* values in the volcanic and the tectonic areas, respectively. Solid bars show standard deviation.

the Hida region, and the Kamitakara Observatory. The hypocenters determined by the Kamitakara Observatory are very accurate. We, therefore, used the hypocenters and origin times which were determined by the Kamitakara Observatory rather than SWARMS. The seismic signals of the vertical component were recorded with 1 Hz velocity-type seismometers whose overall frequency characteristics have a flat response to ground velocity at frequencies of $1 \sim 30$ Hz. The wave forms of earthquakes were recorded at the sampling rate of 100 Hz through an A/D converter and a mini-computer by SWARMS.

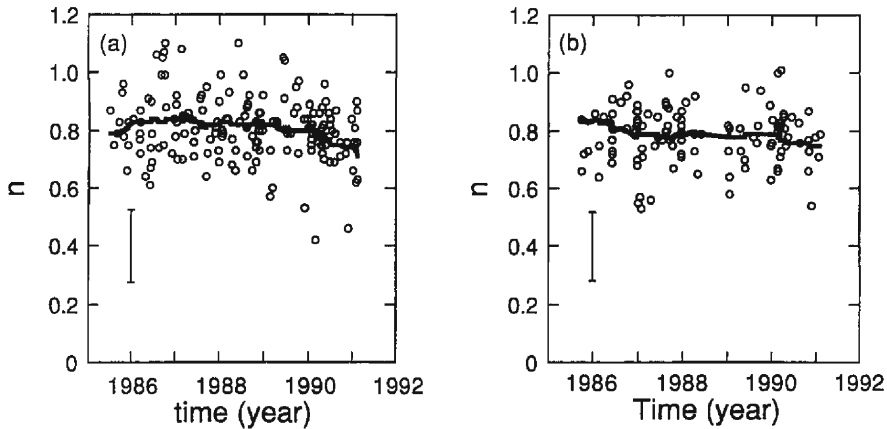We selected the earthquakes that satisfied the following conditions:

Fig. 8. (a) and (b) indicate temporal variations in the power of frequency n for coda Q^{-1} in the volcanic and the tectonic areas, respectively. Solid curve is running mean of 21 successive data and solid bars show standard deviation from the running mean.
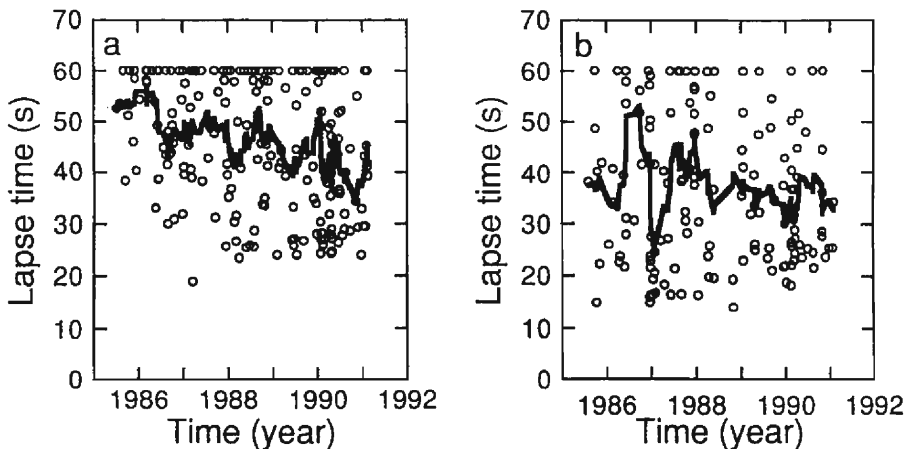

Fig. 9. (a) and (b) indicate temporal variations in the end of lapse time used to estimate coda Q^{-1} in the volcanic and the tectonic areas, respectively. Solid curve is running mean of 11 successive data.
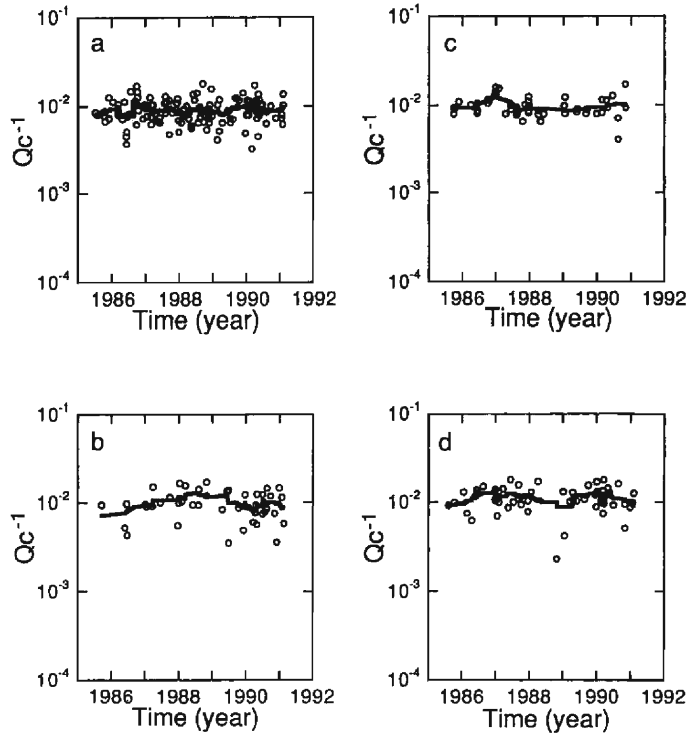
Fig. 10. (a) and (b) indicate temporal variations in coda Q^{-1} of 1.5 Hz in the volcanic area for lapse time in excess of 40 s and within 40 s, respectively. (c) and (d) indicate temporal variations in coda Q^{-1} of 1.5 Hz in the tectonic area for lapse time in excess of 40 s and within 40 s, respectively. Solid curve is running mean of 11 successive data.

Table 3. The values of coefficients c and d in Equation (6).

	1.5 Hz	3.0 Hz	6.0 Hz	12.0 Hz	24.0 Hz
Volcanic area					
$c\ (\times 10^{-3})$	12.8	6.10	3.14	2.27	1.47
$d\ (\times 10^{-5})$	7.20	3.98	1.35	1.31	1.16
Tectonic area					
$c\ (\times 10^{-3})$	12.7	5.02	2.83	2.08	1.38
$d\ (\times 10^{-6})$	52.5	5.89	2.76	6.30	7.45

Table 4. The ratio of increase rate of Q_c^{-1} observed in this study versus that obtained from the change in lapse time at $3.0 \sim 24.0$ Hz in the volcanic area.

Frequency band	Ratio
3.0 Hz	1.78
6.0 Hz	3.18
12.0 Hz	3.41
24.0 Hz	2.79

(1) The events occurred within 80 km from the three stations, and during the period from July 1985 to February 1991. In this period, no major earthquakes and eruptions had ever occurred, but earthquake swarms had continuously occurred.

(2) Focal depths were shallower than 30 km. Most of the earthquakes in the Hida region occurred above this depth, mostly at $0 \sim 10$ km.

(3) Magnitudes were less than 4.0.

These earthquakes were generally the strike-slip type with similar focal mechanisms. Since the maximum recording length of SWARMS is 3 minutes for an earthquake, equivalent to the duration of an earthquake with a magnitude of M 4.1, we refrained from using the earthquakes with magnitudes greater than 4.0.

Figure 2 shows the epicentral distribution of these earthquakes and the location of the stations. The epicenters are grouped into two areas. We call the east part of the Hida region a volcanic area and the west part a tectonic area. The Hida mountain range which includes active volcanoes is located in the volcanic area. On the other hand, many Quaternary faults are distributed in the tectonic area. Earthquake swarms often occur in both areas and the location of their activity moved with time. The earthquakes in the volcanic area are shallower in general than those in the tectonic area. The local variations in focal depth can be interpreted as the difference in the depth of the brittle-ductile transition zone[14].
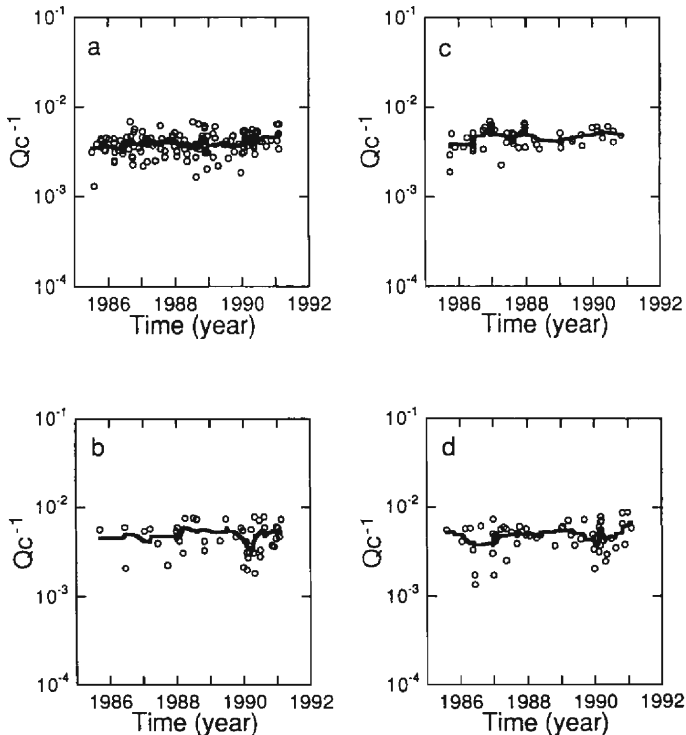

Fig. 11.   Temporal variations in coda Q^{-1} of 3.0 Hz. All symbols are the same as those in Fig. 10.

3.   Method

To estimate the value of coda Q^{-1}, we used the single back scattering model[4].   If the coda amplitude for the central frequency f_0 at lapse time t from the origin time, $A(f_0|t)$, is approximated by the root mean square value, and the lapse time t is greater than twice the travel time of S wave T_S,

$$A(f_0|t) = C(f_0)t^{-a}\exp(-\pi f_0 t/Q_c), \tag{1}$$

where C is the source factor, and a is the geometrical spreading factor, with $a=0.5$ for surface waves and $a=1$ for body waves.   If the natural logarithm is taken, equation (1) gives

$$\ln A(f_0|t) = \ln C(f_0) - a\ln t - bt, \tag{2}$$

where

$$b = \pi f_0 Q_c^{-1}. \tag{3}$$

We assume that coda waves consist of S to S backscattered waves[2], therefore we take $a=1$.

We used the band-pass filtered data, for central frequencies 1.5, 3.0, 6.0, 12.0 and
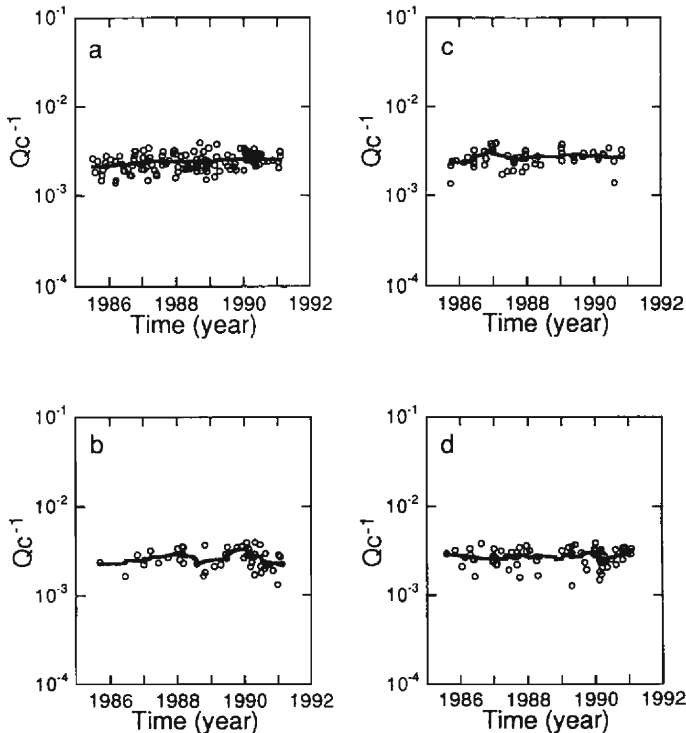

Fig. 12.   Temporal variations in coda Q^{-1} of 6.0 Hz.   All symbols are the same as those in Fig. 10.

24.0 Hz, then calculated the root mean square for moving window for twice the period corresponding to each central frequency. The value of b can be determined from the slope of $t \cdot \ln A(f_0|t)$ versus lapse time for each frequency band by the least squares method. Then the value of Q_C^{-1} was calculated from equation (3).

The time window was taken from twice T_S to 60 s from the origin time, or to the end of the record (at which some reach the ground noise level, while others do not). When the S arrival was not clear, the travel time of the S wave was calculated from the travel time of the P wave by assuming $V_P/V_S = \sqrt{3}$.

In order to determine the value of n, we fit the power law of frequency for Q_C^{-1} as

$$Q_C^{-1} = Q_0^{-1} f^{-n}, \tag{4}$$

where Q_0^{-1} is the Q_C^{-1} at 1 Hz. The above formula is fitted by the least squares method.

4. Result

We adopted the method introduced in the preceding section for analyzing 367 local earthquakes. **Figures 3** and **4** show temporal changes in Q_C^{-1} for five frequency bands in the volcanic area and the tectonic area, respectively. The values of Q_C^{-1} seemed to in-
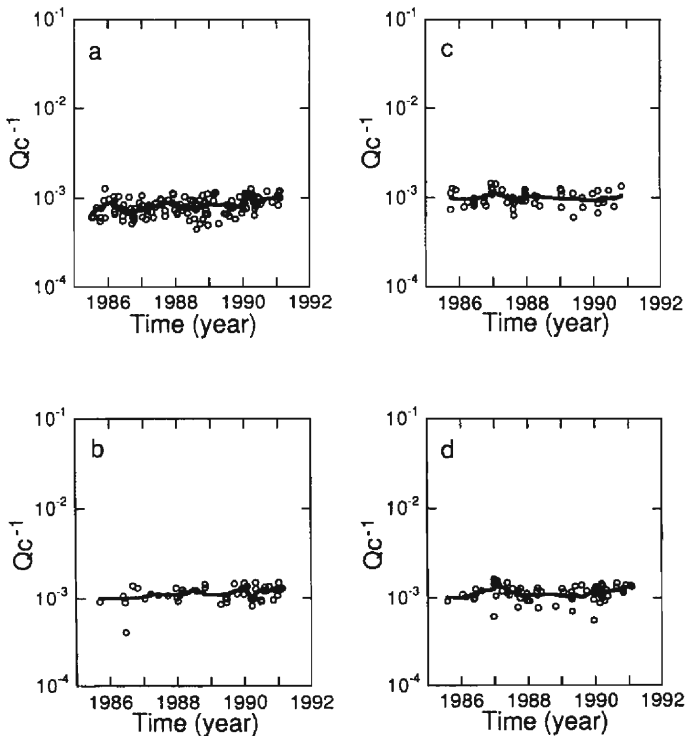

Fig. 13.   Temporal variations in coda Q^{-1} of 12.0 Hz.   All symbols are the same as those in Fig. 10.

crease gradually with time in the volcanic area. The tendency of increase in $Q_C{}^{-1}$ was remarkable for the high frequency bands. The temporal variation in $Q_C{}^{-1}$, however, was not clear in the tectonic area.

We also examined statistically temporal change in $Q_C{}^{-1}$. The studied $Q_C{}^{-1}$ values are divided into three periods, (I) Jul. 1985 ~ May 1987, (II) Jun. 1987 ~ Apr. 1989 and (III) May. 1989 ~ Feb. 1991. The mean value of $Q_C{}^{-1}$ for each period and the results of Student's t test are shown in **Table 2**. The value of significance shows the probability of occurrence of the difference in two sample means under the assumption that population means are equal. A small value of the significance, which is taken to be less than 5% in this study, indicates that the observed difference is quite significant. The mean value increased for all frequency bands with time in the volcanic area. By the t test, the difference in the means of $Q_C{}^{-1}$ between (I) and (II) is significant for 3.0 ~ 24.0 Hz bands. While in the tectonic area, the mean value does not always increase with time for each frequency band. Small values of significance were also seen for high frequency bands in the tectonic area. The mean values decreased from (I) to (II) and increased from (II) to (III). The scatter of data in the latter half of 1988 may have caused such changes. However, the change in the mean value from (I) to (III) is not significant. We cannot judge whether $Q_C{}^{-1}$ for about 5 years in the tectonic area increased or decreased. Therefore, we consider that the temporal variation in $Q_C{}^{-1}$ in the tectonic
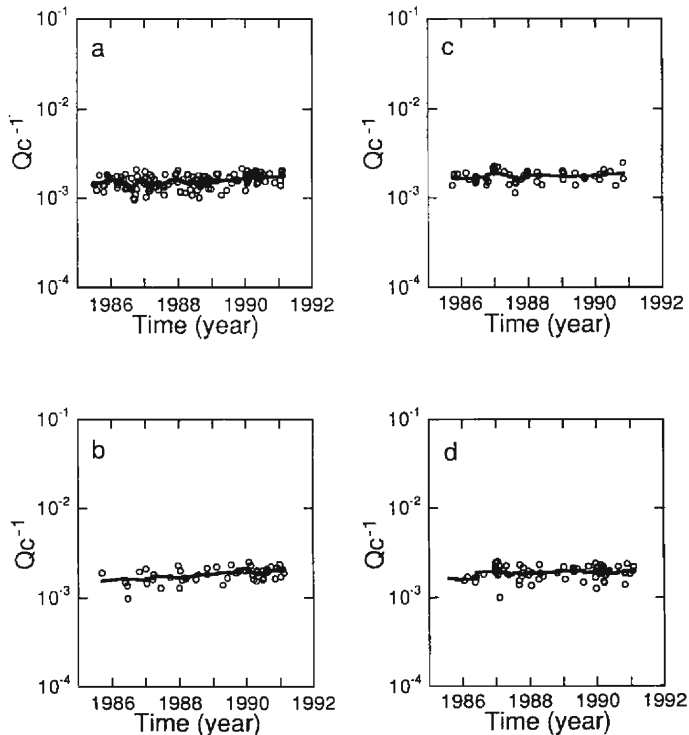

Fig. 14. Temporal variations in coda Q^{-1} of 24.0 Hz. All symbols are the same as those in Fig. 10.

area is not significant. To make our discussion certain, we have dealt with temporal change in Q_C^{-1} only in the volcanic area.

Next we examined the temporal change in the number of earthquakes in the Hida region. As shown in **Figure 2**, earthquakes with magnitudes greater than or equal to 1.5 were observed at all stations in the Hida region in order to exclude the influence of small earthquakes detected at each station. **Figure 5** shows the temporal variation of monthly numbers of earthquakes in the volcanic and the tectonic areas. In this figure, high peaks correspond to the occurrence of earthquake swarms. The original activity of earthquakes in the volcanic area was higher than that in the tectonic area. The number of earthquakes increased with time in the volcanic area, but was uniform with time in the tectonic area. We, however, could not find a remarkable change in Q_C^{-1} in the volcanic area related to earthquake swarms which correspond to high peaks in **Figure 5** as, for example, occurred in 1990 in the Hida mountain range. Q_C^{-1} is considered to be a reliable indicator of stress condition[3], but we could not immediately determine if the stress change occurred locally within the volcanic area or widely over the Hida region. Since the lapse time used to estimate Q_C^{-1} was long, the path of coda waves could not be separated strictly into two areas by the location of the hypocenter. The temporal change in Q_C^{-1} observed in this study may represent the mean value of Q_C^{-1} in the Hida region and may not reflect local stress change. The results of the statistical test, however, revealed the temporal variation in Q_C^{-1} in the volcanic area was significant and that in
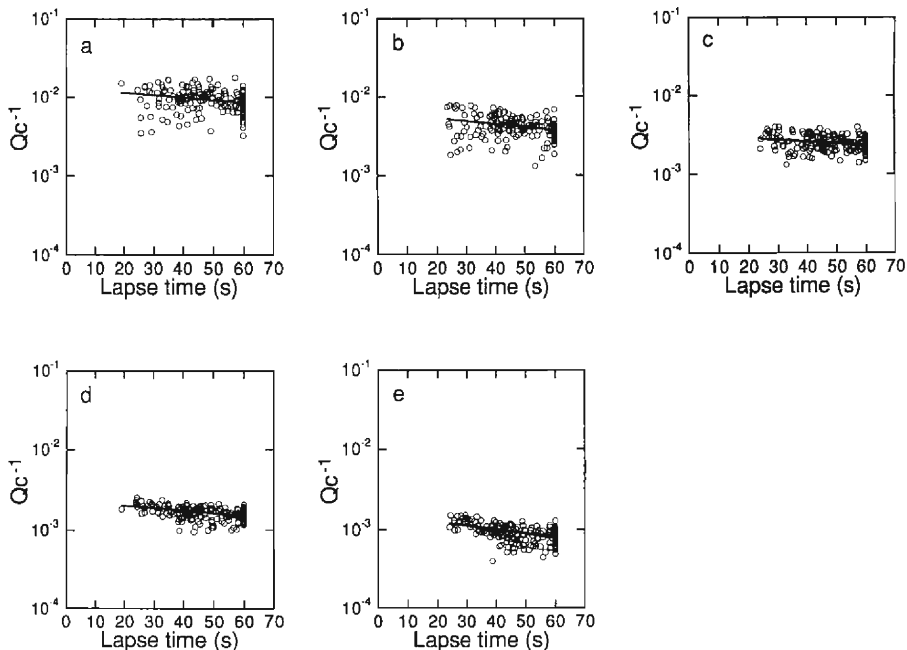

Fig. 15. (a), (b), (c), (d) and (e) indicate distribution of coda Q^{-1} versus lapse time in the volcanic area at 1.5, 3.0, 6.0, 12.0 and 24.0 Hz, respectively. Solid line is linear trend fitted by the least squares method.

the tectonic area was not.   There is, however, a possibility that micro-earthquakes occur beneath the Hida mountain range because of wide variation of the stress level.   The ductile portions are more sensitive to the change in stress level than the brittle portions.   The deformation in the ductile portions of lithosphere occurs aseismically and plays a major roll in loading the brittle portions[11].   Since the brittle-ductile transition depth is shallower beneath the Hida mountain range than beneath the Atotsugawa falut[14], seismicity and crack density may be enhanced in the volcanic area due to the lesser strength of the lithosphere.

The *b* value was determined by fitting the following formula:

$$\log N(M) = a - bM, \tag{5}$$

where *M* is the magnitude and *N(M)* represents total number of earthquakes with magnitudes in excess of *M*.   We counted *N(M)* for 12 months successive every 3 months with a magnitude increment of 0.1.   A straight line was fitted to magnitude frequency distribution in the magnitude range of $1.5 \sim 4.0$ by the least squares method (**Figure 6**). **Figure 7** shows the temporal variation in *b* value in the volcanic area and the tectonic area.   In the volcanic area, the *b* value increased from the middle of 1985 to the middle of 1987, and was almost constant in the rest period.   But through our analysis period, we observed that the *b* value increased with time.   In the tectonic area, from 1986 to early 1990 the *b* value increased with time, but decreased suddenly toward 1991.
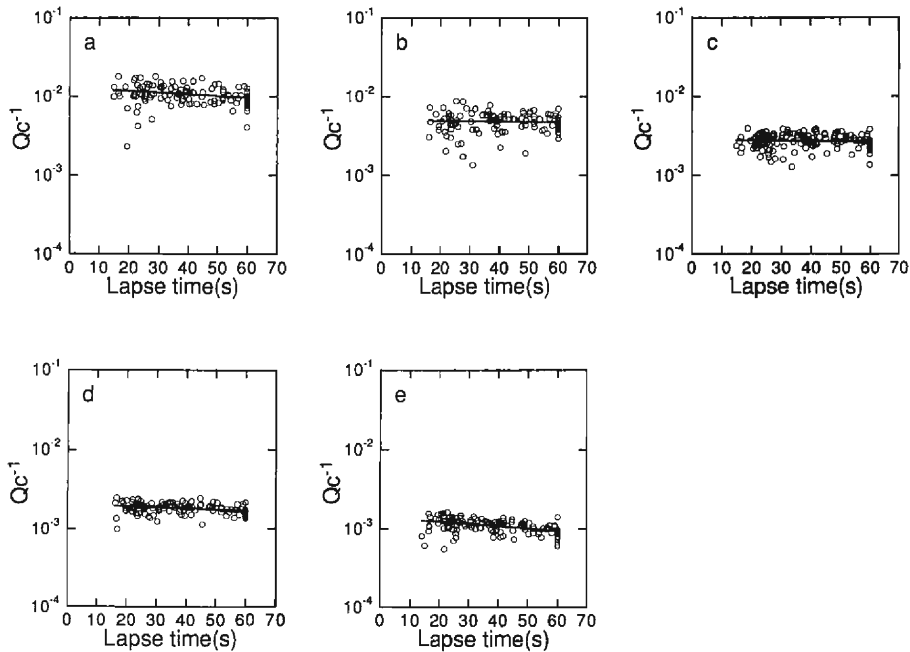

Fig. 16.   (a), (b), (c), (d) and (e) indicate distribution of coda Q^{-1} versus lapse time in the tectonic area at 1.5, 3.0, 6.0, 12.0 and 24.0 Hz, respectively.   Solid line is linear trend fitted by the least squares method.

The frequency dependence of Q_C^{-1} was also examined.　**Figure 8** shows the temporal changes in the value of frequency dependence n in the volcanic and the tectonic areas.　We recognized no significant systematic change in n.　In both areas, most values of n were in the range of $0.6 \sim 1.0$ which was relatively high.　These values of n are similar to those of the eastern and central Kanto region in Japan[2], central California[16] and Adak Island area, central Aleutians[28] (See **Table 1.**).　This result clearly shows that the value of n is large in a tectonically active region, such as the Hida region.

5.　Discussion

The apparent changes in coda Q^{-1} are caused by any systematic change in the focal mechanism, the epicenters and focal depth, and the selected time window[25].　First, we examined the possibility that the observed changes in coda Q^{-1} were not due to these causes.

Different time windows, in general, yield different values of Q_C^{-1}.　The value of Q_C^{-1} tends to be smaller at long lapse time than that at short lapse time.　The end of the time window used in this study varies depending on the earthquake magnitude.　The time windows for the present analysis are summarized in **Figure 9**.　Since the average lapse time was shortest in 1990, the average lapse time seemed to decrease with time, although most of the time-window ends are in the range of $40 \sim 60$ s in the volcanic area.　To iden-
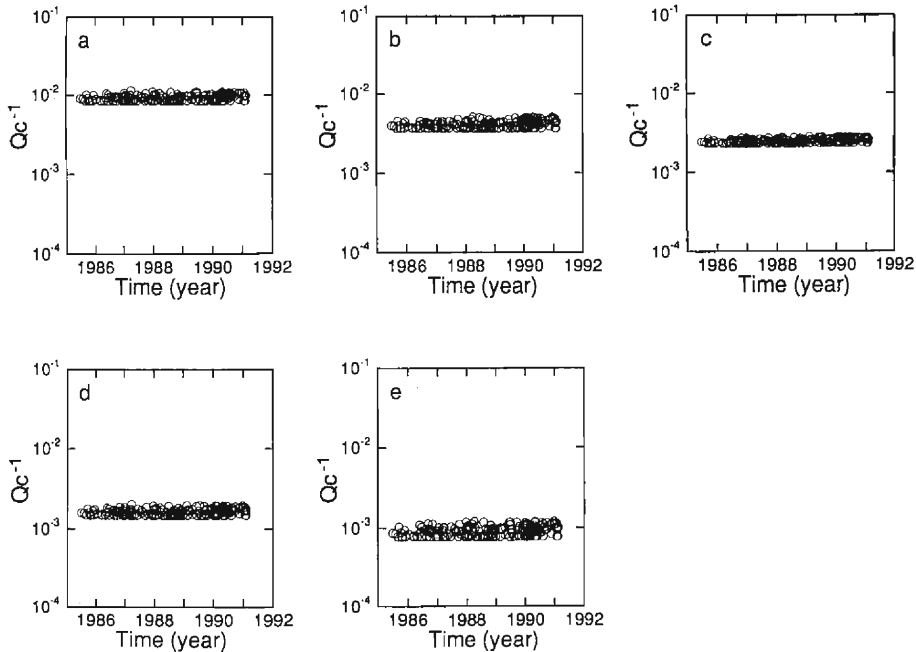

Fig. 17.　(a), (b), (c), (d) and (e) indicate temporal variations in coda Q^{-1}, which obtained by Equation (6), due to temporal variations in lapse time in the volcanic area at 1.5, 3.0, 6.0, 12.0 and 24.0 Hz, respectively.　Coefficients c and d are given in Table 3.

tify the effect of time windows on the temporal variation in Q_C^{-1}, we separated the data of Q_C^{-1} into two groups: lapse times above 40 s and those below 40 s (**Figures 10~14**). We found, at least, a similar trend both groups of lapse times above and below 40 s in the volcanic area. **Figures 15** and **16** show the lapse time dependence of Q_C^{-1} in the volcanic and tectonic areas, respectively.

We also tested the possibility that the temporal variation in Q_C^{-1} was all caused by variation in lapse time. We assume that a linear relation,

$$Q_C^{-1} = c - dt, \tag{6}$$

where t is the end of lapse time. The coefficients c and d are given in **Table 3**. The temporal variations in Q_C^{-1} due to the change of lapse time were obtained as shown in **Figures 17** and **18**. Nevertheless, we could not recognize the temporal variation in Q_C^{-1} due to the change of lapse time equal to the temporal variation in Q_C^{-1} shown in **Figures 3** and **4**. Further, the linear trends of the temporal variations in Q_C^{-1} were examined. In fact, the rates of increase in Q_C^{-1} with time for 6.0, 12.0 and 24.0 Hz frequency bands in the volcanic area, in which the temporal variations in Q_C^{-1} are significant by statistical test, are more than about three times as large as those expected from the lapse time—Q_C^{-1} relation (**Equation 6**). For the 3.0 Hz band, the observed trend is only 1.7 times larger than expected value (**Table 4**). The temporal variation in Q_C^{-1} at 3.0 Hz may have been the change in lapse time. We, however, could not explain the
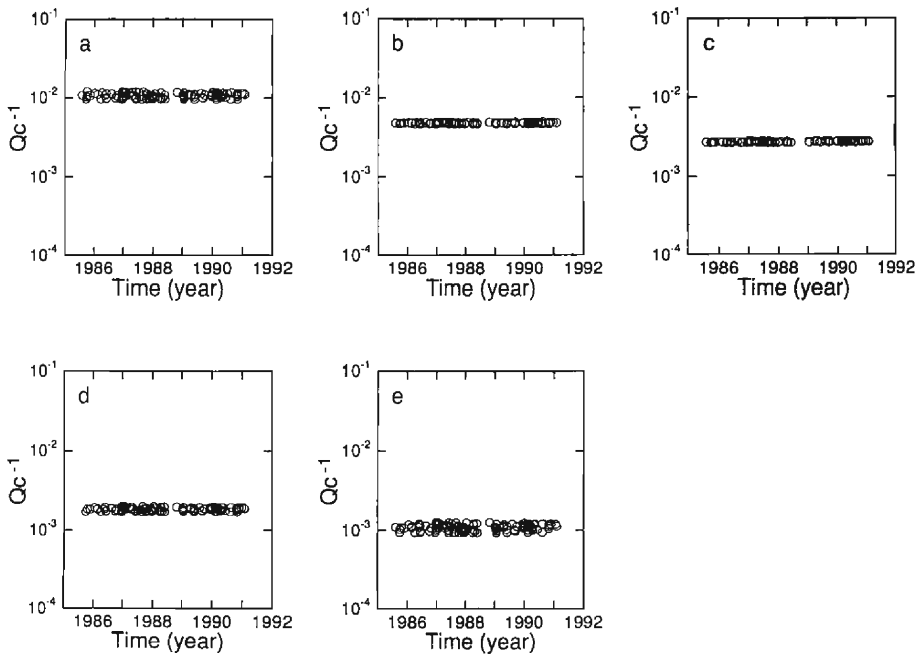

Fig. 18. (a), (b), (c), (d) and (e) indicate temporal variations in coda Q^{-1}, which obtained by Equation (6), due to temporal variations in lapse time in the tectonic area at 1.5, 3.0, 6.0, 12.0 and 24.0 Hz, respectively. Coefficients c and d are given in Table 3.

temporal variation in $Q_C{}^{-1}$ at $6.0 \sim 24.0$ Hz in the volcanic area by the temporal change in lapse time.

The effect of focal depth can be considered, because a systematic change in $Q_C{}^{-1}$ with focal depth had been observed[30)20]. These results show that a change in focal depth of about 100 km is required to explain the observed change in $Q_C{}^{-1}$. All earthquakes used in this study are shallower than 30 km, probably 15 km, and errors in focal depth of as much as 100 km are impossible.

The change in the focal mechanism affects the early part of S coda[22]. The focal mechanisms of earthquakes involved were generally strike-slip both in the volcanic and the tectonic areas[14]. No remarkable change in the focal mechanism was detected for the period of our coda Q^{-1} analysis. From the above considerations, the temporal change or trend in $Q_C{}^{-1}$ is not apparent change.

As mentioned in the Introduction, temporal changes in $Q_C{}^{-1}$ were generally related to major earthquakes and eruptions in many reports[6)18)8)31)10)23]. No major earthquakes and eruptions, however, had occurred in this study area during the period of the present analysis. Therefore, it seems that the increase found in coda attenuation was not precursor to a large earthquake; such a change is most likely to be caused by aseismic fracture, increasing scatter on creeping cracks, beneath and around the Hida mountain range.

Jin and Aki[11] proposed that aseismic creep activities tend to increase the crack density and coda Q^{-1} in a seismic region. The positive correlation between $Q_C{}^{-1}$ and b value in the volcanic area is considered that the characteristic magnitude M_C is $1.5 < M_C < 2.0$ and creep scale length is small, which enhances seismicity of earthquakes with magnitude corresponding to $1.5 < M_C < 2.0$.

The increase in b value is caused by the relative increase in the number of small earthquakes or decrease in that of large earthquakes in the range used to estimate b values. **Figure 19** shows the temporal variations in the cumulative number of earthquakes for 12 successive months, which are in the range of $1.5 \sim 2.0$ and $3.5 \sim 4.0$ with magnitudes, used to determine b values in the volcanic area. The temporal variation in the number of events with a magnitude range of $3.5 \sim 4.0$ is smaller than that of the $1.5 \sim 2.0$ events. We, therefore, recognized that the variations in the number of small events with magnitudes $1.5 \sim 2.0$ were dominant in the variations in b value. If the scale of magnitude directly relates to the length of the earthquake rupture, the increase in $Q_C{}^{-1}$ for higher frequency bands can be attributed to the increase in small cracks since the scattering is more effective when the wavelength nearly corresponds to the scale of a crack.

In the Hida region, low velocity bodies exist beneath the active volcanoes in the crust and the upper mantle which may be partially melted[9]. Since most of the ends of time windows are in a range of 40 to 60 s from an origin time, the coda waves used in this study had enough time to sample the low velocity bodies. The value of $Q_C{}^{-1}$, therefore, could have been greatly affected by these bodies. The difference of the temporal variation in $Q_C{}^{-1}$ between the volcanic area and the tectonic area may reflect the degree of sampling of these low velocity bodies. These bodies may be a source of magma of the volcanoes located in the Hida mountain range. We can consider that magma transporta-
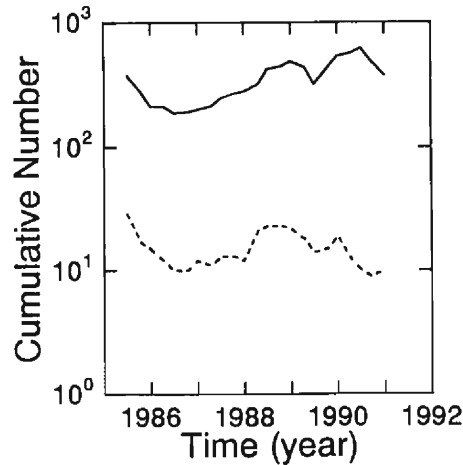
Fig. 19. Temporal variation in cumulative number of earthquakes for 12 successive months in the volcanic area. Solid curve shows the variation in number of earthquakes with magnitudes range of 1.5~2.0. Dashed curve shows the variation in number of earthquakes with magnitude range of 3.5~4.0.

tion has continued steadily in the lithosphere with consequently rearranged scattered environments. This magma movement enhances creep activity in the ductile portion of the lithosphere. The increase in Q_C^{-1} reflects the process of the magma accumulation. The activity of earthquake swarms can be expected to be directly related to volcanism rather than tectonic movements. For example, the earthquake swarms in southeast of Mt. Ontake (October 1978) were more or less affected by the October 28, 1979 volcanic eruption of Mt. Ontake. A series of earthquake swarms and the observed temporal changes in Q_C^{-1} are possibly linked through the phenomenon of magma transportation.

In the volcanic area, as mentioned in the Data, the brittle portions are much smaller than the ductile portion within the lithosphere. We can interpret, therefore, that the temporal change in Q_C^{-1} is attributable to aseismic fracture, that may be related to magma accumulation in the ductile portion of the lithosphere.

6.   Conclusion

Coda Q^{-1} was measured for earthquakes located in the Hida region, central Japan, using single backscattering model of coda generation. The values of coda Q^{-1} are increasing with time in the volcanic area at higher frequency bands. The power of frequency for coda Q^{-1} was found in the range of 0.6~1.0. These are typical values in tectonically active regions. Positive correlation was found between coda Q^{-1} and b values in the volcanic area. The existence of low velocity bodies beneath the Hida mountain range and large volume of ductile portions in the lithosphere markedly affects the changes in coda Q^{-1} and seismicity. Since major earthquakes and eruptions never occurred in the Hida region during our analysis period, we can consider that the observed

temporal changes reflect aseismic phenomena in the lithosphere. We can interpret, therefore, that the temporal changes in coda Q^{-1} are caused by the aseismic fractures associated with magma accumulation. The earthquake swarms around and beneath the Hida Mountain range may also be related to magma accumulation.

Acknowledgements

References

1) Aki, K.: Analysis of the seismic coda of local earthquakes as scattered waves. J. Geophys. Res., Vol. 74, 1969, pp. 615–631.

2) Aki, K.: Scattering and attenuation of shear waves in the lithosphere. J. Geophys. Res., Vol. 85, 1980, pp. 6496–6504.

3) Aki, K.: Theory of earthquake prediction with special reference to monitoring of the quality factor of the lithosphere by the coda method. Earthq. Predict. Res., Vol. 3, 1985, pp. 219–230.

4) Aki, K. and Chouet, B.: Origin of coda waves: source, attenuation and scattering effects. J. Geophys. Res., Vol. 80, 1975, pp. 3322–3342.

5) Chouet, B.: Temporal variation in the attenuation of earthquake coda near Stone Canyon, California. Geophys. Res. Lett., Vol. 6, 1979, pp. 143–146.

6) Del Pezzo, E., Ferulano, F., Giarrusso, A. and Martini, M.: Seismic coda, Q and scaling law of the source spectra at the Aeolian Islands, southern Italy. Bull. Seism. Soc. Am., Vol. 73, 1983, pp. 97–108.

7) Disaster Prevention Research Institute, Kyoto University.: Seismic Wave Automatic Processing System at Disaster Prevention Research Institute, Kyoto University Report of the Coordinating Commitee for Earthquake Predection, Vol. 35, 1986, pp. 431–436. (in Japanese)

8) Gusev, A. A. and Lemzikov, V. K.: Properties of scattered elastic waves in the lithosphere of Kamchatka: Parameters and temporal variations. Tectonophysics, Vol. 112, 1985, pp. 137–153.

9) Hirahara, K., Ikami, A., Ishida, M. and Mikumo, T.: Three-dimensional P-wave structure beneath central Japan: low velocity bodies in the wedge portion of the upper mantle above high-velocity subducting plates. Tectonophysics, Vol. 163, 1989, pp. 63–73.

10) Jin, A. and Aki, K.: Temporal change in coda Q before the Tangshan earthquake of 1976 and the Haicheng earthquake of 1975. J. Geophys. Res., Vol. 91, 1986, pp. 665–673.

11) Jin, A. and Aki, K.: Spatial and temporal correlation between coda Q^{-1} and seismicity and its physical mechanism. J. Geophys. Res., Vol. 94, 1989, pp. 14041–14059.

12) Jin, A., Cao, T. and Aki, K.: Regional change of coda Q in the ocean lithosphere. J. Geophys. Res., Vol. 90, 1985, pp. 8651–8659.

13) Kamitakara Crustal Movement Observatory, Disaster Prevention Research Institute, Kyoto University.: Recent Swarm Earthquakes beneath the Hida Mountain Range. Report of the Coordinating Commitee for Earthquake Predection., Vol. 44, 1990, pp. 339–348. (in Japanese)

14) Mikumo, T., Wada, H. and Koizumi, M.: Seismotectonics of the Hida region, central Honshu, Japan. Tectonophysics, Vol. 147, 1988, pp. 95–119.

15) Pulli, J. J.: Attenuation of coda waves in New England. Bull. Seism. Soc. Am., Vol. 74, 1984, pp. 1149–1166.

16) Phillips, W. S., Lee, W. H. K. and Newberry, T.:   Spatial variation of crustal coda Q in California. Pure Appl. Geophys., Vol. 128, 1988, pp. 251–260.

17) Rautian, T. G. and Khalturin, V. I.:   The use of coda for determination of the earthquake source spectrum. Bull. Seism. Soc. Am., Vol. 68, 1978, pp. 923–948.

18) Rhea, S.: Q determined from local earthquakes in the South Carolina coastal plain. Bull. Seism. Soc. Am., Vol. 74, 1984, pp. 2257–2268.

19) Robinson, R.:   Temporal variation in coda duration of local earthquakes in the Wellington region, New Zealand. Pure Appl. Geophys., Vol. 125, 1987, pp. 579–596.

20) Roecker, S. W., Tucker, B., King, J. and Hatzfeld, D.:   Estimates of Q in central Asia as a function of frequency and depth using the coda of locally recorded earthquakes. Bull. Seism. Soc. Am., Vol. 74, 1984, pp. 2257–2268.

21) Rovelli, A.:   On the frequency dependence of Q in Friulli from short-period digital records. Bull. Seism. Soc. Am., Vol. 72, 1982, pp. 2369–2372.

22) Sato, H.:   Attenuation of envelope formation of three-component seismograms of small local earthquakes in randomly inhomogeneous lithosphere. J. Geophys. Res., Vol. 89, 1984, pp. 1221–1241.

23) Sato, H.:   Temporal change in attenuation intensity before and after the eastern Yamanashi earthquake of 1983, in central Japan. J. Geophys. Res., Vol. 91, 1986, pp. 2049–2061.

24) Sato, H.:   A precursorlike change in coda excitation before the Western Nagano Earthquake (Ms = 6.8) of 1984 in central Japan. J. Geophys. Res., Vol. 92, 1987, pp. 1356–1360.

25) Sato, H.:   Temporal change in scattering and attenuation associated coda waves—A review of recent studies on coda waves. Pure Appl. Geophys., Vol. 126, 1988, pp. 465–498.

26) Scherbaum, F. and Kisslinger, C.:   Coda Q in the Adak seismic zone. Bull. Seism. Soc. Am., Vol. 75, 1985, pp. 615–620.

27) Singh, S. and Herrmann, R. B.:   Regionalization of crustal coda Q in the continental United States. J. Geophys. Res., Vol. 88, 1983, pp. 527–538.

28) Steensma, G. J. and Biswas, N. N.:   Frequency dependent characteristics of coda wave quality factor in central and southcentral Alaska. Pure Appl. Geophys., Vol. 128, 1988, pp. 295–307.

29) Takayama Seismological Observatory, School of Science, Nagoya University.:   Recent seismic activity to the south of Mt. Norikura (May 1, 1989 ~ May 17, 1990). Report of the Coordinating Committee for Earthquake Prediction, Vol. 44, 1990, pp. 329–332. (in Japanese.)

30) Tsujiura, M.:   Spectral analysis of the coda waves from local earthquakes. Bull. Earthquake Res. Inst., Tokyo Univ., Vol. 53, 1978, pp. 1–48.

31) Tsukuda, T.:   Coda-Q before and after the 1983 Misasa earthquake of M 6.2, Tottori Prefecture, Japan. Pure Appl. Geophys., Vol. 128, 1988, pp. 261–279.